Remarkable effects of uniaxial stress on the far-infrared laser emission in p-type Ge

S. Komiyama and S. Kuroda
Department of Pure and Applied Sciences, University of Tokyo, Komaba, Tokyo 153, Japan
(Received 19 August 1987)

The influence of [112] compressive stress on the inter-valence-band laser emission from a p-type Ge crystal containing the acceptor concentration $N_a \simeq 6\times10^{13}$ cm^{-3} is studied. In the absence of stress, the laser emission is classified to the longer-wavelength oscillation ($\lambda \gtrsim 170$ μm) in lower electric fields ($E \lesssim 800$ V/cm) and the shorter-wavelength oscillation ($\lambda \lesssim 120$ μm) in higher electric fields ($E \gtrsim 800$ V/cm). At stress magnitudes of 300 ± 70 and 450 ± 80 kg/cm^2, the electric field range for the laser oscillation is significantly extended to lower fields, and the intensity of the laser emission in the lower electric fields ($E \lesssim 800$ V/cm) increases by a factor of $10-10^3$. Further, at stress magnitude 450 ± 80 kg/cm^2, new emission lines appear in the intermediate range of λ (120–170 μm), where the oscillation is missing in zero stress. The experimental results are interpreted in terms of the reduction of the rate of inter-valence-band impurity scattering under uniaxial stress.

I. INTRODUCTION

Since the discovery of the inter-valence-band far-infrared laser oscillation in p-type Ge,[1] its fundamental characteristics have been studied, such as the emission spectra,[2–6] the light polarization,[5,7] the output power,[1,8,9] and the gain coefficient.[9,10] Aside from these studies it is of particular interest to study the influence of uniaxial stress on the laser oscillation, since the uniaxial stress is known to remove the valence-band degeneracy in Ge[11] and an enhancement of the light-hole accumulation is thereby expected.

In this work we have applied [112] compressive stress on a p-type Ge sample up to a magnitude of 450 kg/cm^2. As expected, we have found the characteristics of the laser oscillation to be improved remarkably in several respects. We have briefly reported part of the experimental results in Ref. 5. Here we report the results in more detail along with the interpretation.

II. EXPERIMENTAL METHODS

The p-type Ge sample used is a parallelepiped of $5\times4\times60$ mm^3 in size. The end faces of 5×4 mm^2 and the side faces of 5×60 mm^2 are, respectively, normal to the $\langle 111\rangle$ and the $\langle 112\rangle$ directions. The sample is cut out of an ingot containing Ga to a concentration of $N_a \simeq 6.0\times10^{13}$ cm^{-3}. Ohmic contacts are fabricated on the opposite side faces of 4×60 mm^2.[2] The contact faces are indium soldered and covered with copper foils to serve as electrodes. Figure 1 shows the sample head for stress application. A concave mirror M_1 and a mesh mirror M_2 are attached to the opposite ends of the sample to form a semiconfocal resonator. The characteristics of the resonator have been described in Ref. 6. All the parts of the stress jig, i.e., the main holder, the spacer, the cover, and the screws, are made of stainless steel (SUS 304). The sample rod is wrapped with a 6-μm-thick Mylar foil for electrical insulation and placed in the main holder of 53 mm length. The [112] compressive stress is applied to the sample through the 3-mm-thick spacer pushed to the sample by screws S at the 4-mm-thick cover. The cover is screwed to the main holder. To prevent sample failure on the application of stress, the (112) sample faces are ground parallel within 30 sec and polished optically flat. In addition, sheets of patronpaper (Patronenpapier), 0.1-mm thick, are cemented to the bottom of the main holder and the spacer to provide buffers to avoid localized-strain-concentration points. The side walls of the main holder have appropriate holes to assure sufficient heat exchange of the sample. Current leads, which are omitted in Fig. 1, are soldered to the copper electrodes at places near mirror M_1.

To estimate the stress magnitude, the relation between the stress magnitude and the torque value of the screws S is studied at room temperature by inserting a stress-sensor film ("Prescale," Fuji Photo Film Co.) between the

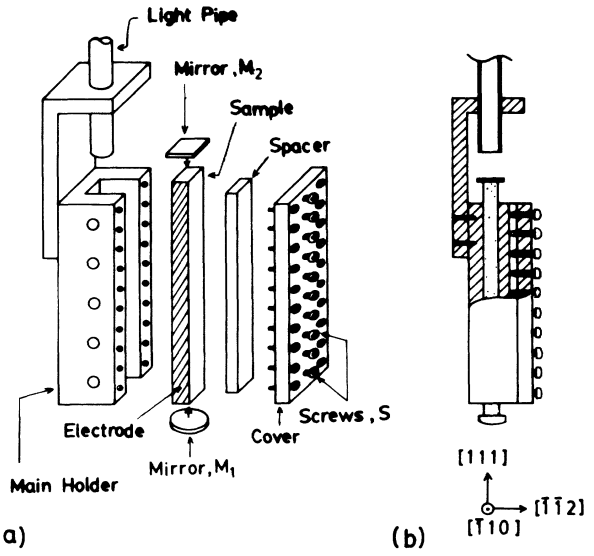

FIG. 1. The sample head for stress application. (a) The parts for the stress jig. (b) The cross section when they are assembled.

sample and the spacer. The sensor film indicates the stress magnitude by its coloring, which is examined by the sight inspection of the sensor film after it is removed from the stress jig. For the experiments, a defined torque is applied to the screws at room temperature and the sample head is then cooled down to helium temperature. After this method, stress magnitude at room temperature is determined with an accuracy of ±15%. The stress magnitude is estimated to increase by 10–20 % at helium temperature when the difference of thermal expansion between the Ge single crystal and the stainless steel is considered. In this way, we have applied two different stress magnitudes, which are estimated to be $F=300\pm70$ and 450 ± 80 kg/cm^2. We will hereafter refer to these stress magnitudes simply as $F=300$ and 450 kg/cm^2 for brevity of the description. The uniformity of the stress over the sample face, which is indicated by the homogeneity of the coloring of the sensor film, is better than ±10%.

The sample head is directly immersed in liquid helium and magnetic fields are applied along the long axis of the sample. Voltage pulses with 1 μs duration are applied at a repetition rate of 2–8 Hz. The laser emission transmitted through mirror M_2 is guided through a brass pipe to a Ge/Sb detector placed in another cryostat, similarly to the previous work.[2,9] For spectroscopic studies a grating monochromator of 100 mm focal length is used with 4 mm slit width.

III. EXPERIMENTAL RESULTS

Prior to the study of the laser emission, influence of the [112] compressive stress on the current-voltage characteristics has been studied. The low-field resistivity ρ and the breakdown electric field E_b for the impact ionization of acceptors, which are, respectively, 3.7 MΩ cm and 2.28 V/cm in the absence of stress, decreased to 2.37 MΩ and 2.10 V/cm at stress magnitude 450 kg/cm^2. When we compare the magnitudes of these reductions directly with the corresponding data obtained for [100] stress,[12,13] disregarding the difference of the stress orientation, $F=320\pm30$ kg/cm^2 is derived. This supports the estimated value, $F=450\pm80$ kg/cm^2, because the [100] stress yields a large valence-band splitting than the [112] stress as will be noted in Sec. IV. At higher electric fields well above E_b, on the other hand, the current-voltage characteristics did not change appreciably in the presence of stress. This is reasonable because (1) the carrier density is unchanged, being nearly equal to the net acceptor concentration when $E \gg E_b$, and (2) the effective-mass tensors and the momentum relaxation times of light and heavy holes do not change significantly at the relatively low-stress magnitudes presently applied.[14]

The intensity of the laser emission is found to increase drastically on the application of stress when electric fields are lower than 800 V/cm. Figure 2 displays the detector signal intensities at $E=570$ V/cm as a function of magnetic field B and shows an example of the remarkable intensification of the emitted radiation. In addition to the intensification, the minimum electric field necessary for the laser oscillation, which is 480 V/cm in zero stress, is reduced to 320 V/cm at stress magnitude 300 kg/cm^2

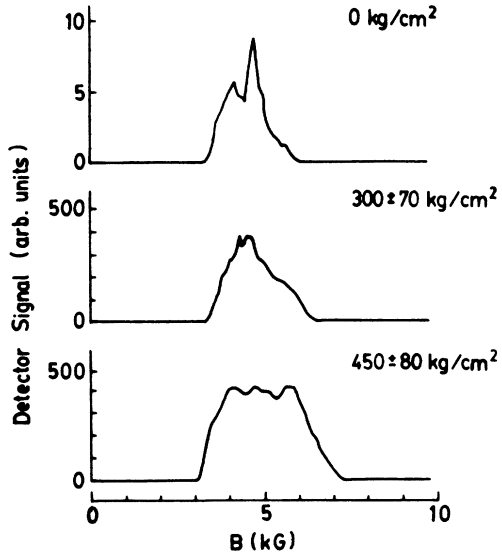

FIG. 2. Influence of [112] stress on the laser emission at $E=570$ V/cm. The scales on the ordinates indicate the relative intensities of the signals.

and to 260 V/cm at 450 kg/cm^2, as will be shown in Fig. 4. In electric fields higher than 1 kV/cm, on the other hand, the emission intensity does not increase appreciably but a pronounced structure appears in the intensity versus B curves as shown for $E=1270$ V/cm in Fig. 3. To illustrate the intensification of the emission in the whole range of electric fields, the maximum signal inten-

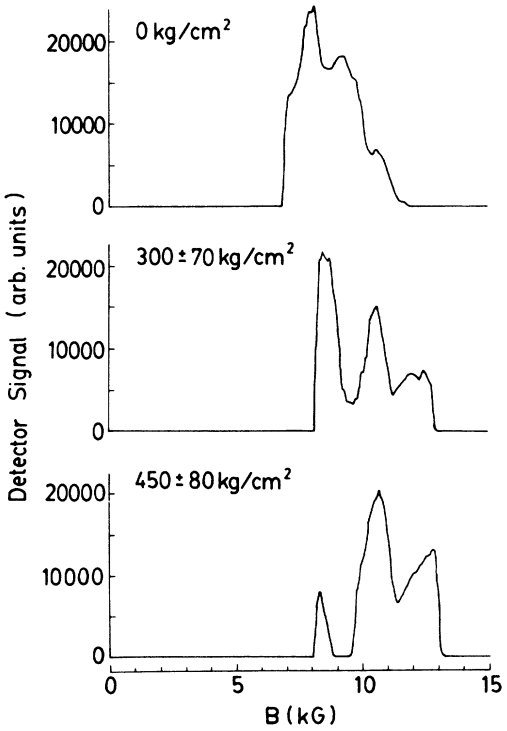

FIG. 3. Influence of [112] stress on the laser emission at $E=1270$ V/cm. The scales on the ordinates indicate the relative intensities of the signals. (The scales are the same as those in Fig. 2.)

sities attained in the sweeps of B are plotted as a function of electric field in Fig. 4.

The stress influences not only the emission intensity but also the wavelength of the emitted radiations as shown in Fig. 5, where the wavelength positions of strong emission lines are plotted as a function of electric field. In the studies of Fig. 5, such magnetic fields were applied as to yield the largest total intensities of the emission at the respective electric fields. The wavelength positions of strong emission lines were, however, found to be substantially independent of magnetic fields. The stress influences also the region of electric and magnetic fields where the oscillation takes place, as shown in Figs. 6 and 7, respectively, for stress magnitudes 300 and 450 kg/cm^2. The regions in Figs. 6 and 7 were determined through the sweeps of B at fixed values of E, where E was varied at intervals of 5–13 %.

We describe below the characteristics of the oscillation in zero stress before examining the influence of stress in detail. Firstly, the oscillation region of E and B develops around the straight line in Figs. 6 or 7, which indicates the relation,

$$\zeta_h \equiv (\hbar k_{\rm op}^h / m_h^*) B/E = 1.3 \ . \tag{1}$$

Here, $m_h^* = 0.35 m_0$ is the effective mass of heavy holes with the free electron mass m_0 and $k_{\rm op}^h$ is defined as

$$k_{\rm op}^h \equiv (2 m_h^* \hbar \omega_{\rm op})^{1/2} / \hbar \tag{2}$$

with the optical phonon energy $\hbar\omega_{\rm op} = 37$ meV. This is reasonable because relation (1) approximately corresponds to the ratio of E and B at which the strongest accumulation of light holes is attained.[1,2,8,9] Second, the oscillations region is clearly divided into two characteristic domains with the border at $E \sim 800$ V/cm and $B \sim 5.5$ kG. In the lower-field domain, the oscillation wavelengths are longer than 170 μm (Fig. 5) and the detector-signal intensities due to the oscillations are relatively low (Fig. 4). In the higher-field domain, on the other hand, the wavelengths are shorter than 120 μm and the signal intensities are much higher. The abrupt increase of the signal intensities at the border $E \sim 800$ V/cm (Fig. 4) is partly ascribed to the characteristics of the Ge/Sb detector, whose spectral responsivity sharply increases for wavelengths shorter than 140 μm,[15,16] and partly ascribed to an increase in the emission intensity. It is to be pointed out for the following considerations that such characteristics of the oscillations as described above are the

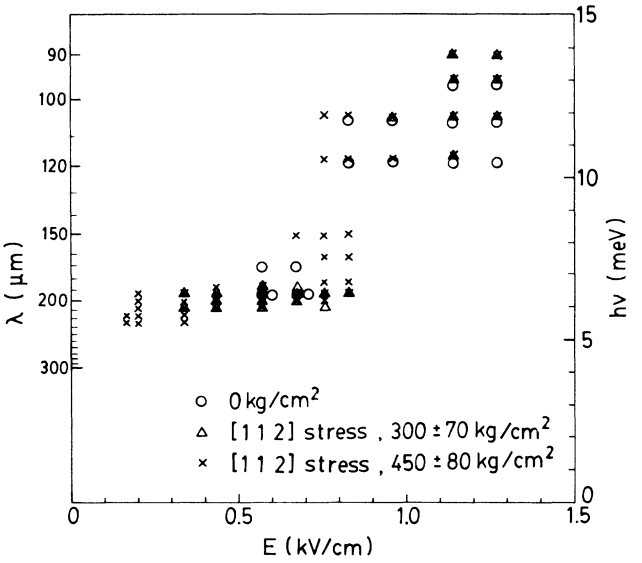

FIG. 5. The wavelengths of strong emission lines as a function of electric field.

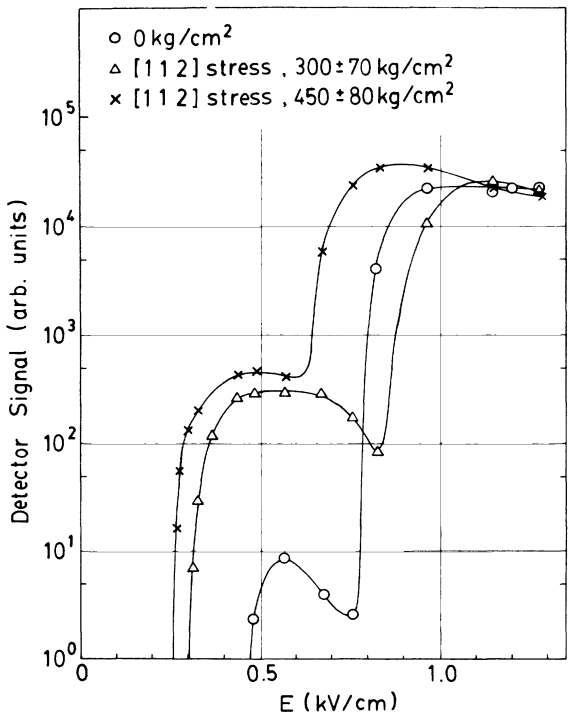

FIG. 4. The signal intensities as a function of electric field.

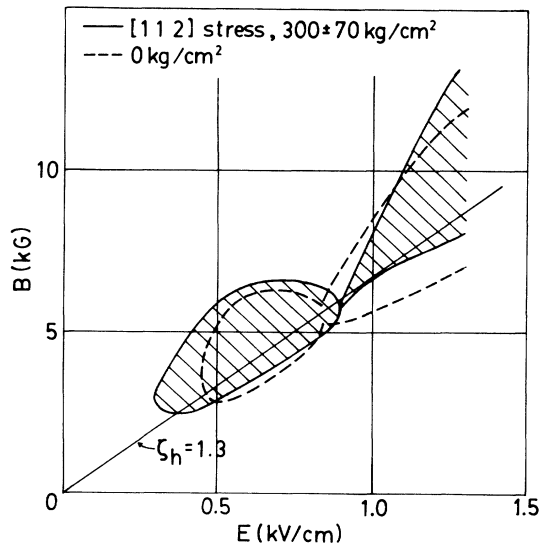

FIG. 6. The region of electric and magnetic fields where the laser oscillation takes place. The region at stress value 300±70 kg/cm^2 (the shaded area) is compared with the region in zero stress bounded by the dashed line.

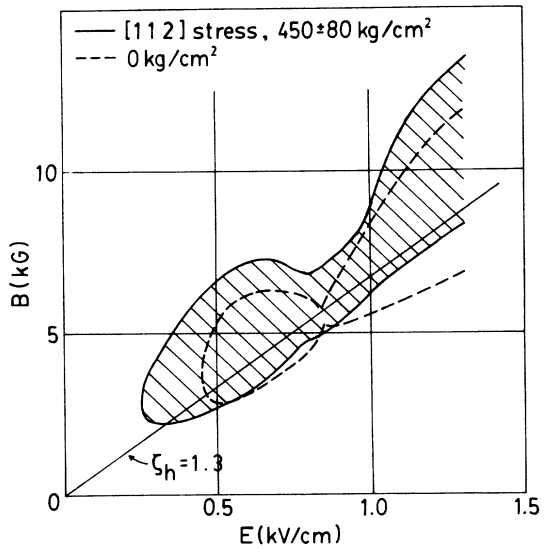

FIG. 7. The oscillation region at stress value 450±80 kg/cm^2 (the shaded area) and that in zero stress (the area bounded by the dashed line).

common features of the oscillation in the absence of stress. It has been observed, independently of the structure of optical resonators, that the oscillation region is divided into the lower- and the higher-field domains, which are characterized, respectively, by the longer-wavelength oscillation ($\lambda > 170$ μm) and the short-wavelength oscillation ($\lambda < 120$ μm) (Refs. 2–6). The oscillation is missing in the intermediate-wavelength range, $120 < \lambda < 170$ μm.[2–6] In the lower-field domain, the oscillation intensity is generally lower than that in the higher-field domain, and it decreases sharply with increasing the acceptor concentration N_a of samples from 3×10^{13} to 1×10^{14} cm^{-3}.[4,17] It has been also observed that the oscillation in the higher-field domain is relatively insensitive to the sample purity.[4,17]

The two domains for oscillation are still discerned at stress magnitude 300 kg/cm^2, but they begin to merge with each other at 450 kg/cm^2 (Figs. 6 and 7). At both stress magnitudes the lower-field domain expands significantly (Figs. 6 and 7) and the emission intensity there increases, remarkably (Fig. 4). At each stress magnitude, the absolute intensity of the oscillation in the lower-field domain is supposed to reach a level comparable to that in the higher-field domain, because a definite gain saturation has been observed in additional time-resolved measurements of the waveform of the pulsed laser emission at $E \sim 500$ V/cm. At each stress magnitude, the signal intensity still increase abruptly at an intermediate E (Fig. 4). It is to be noted that each stress magnitude this abrupt increase coincides with the occurrence of the oscillation line(s) at wavelengths shorter than 150 μm (Fig. 5). Therefore the abrupt increase in the detector-signal intensity is to be primarily ascribed to the characteristic of the spectral responsivity of the detector.

At stress magnitude 300 kg/cm^2, the oscillation wavelengths are still limited to the ranges of $\lambda > 170$ μm and $\lambda < 120$ μm according to the oscillation domains, similarly to the case in zero stress (Fig. 5). At stress magnitude 450 kg/cm^2, however, there appear oscillation lines at $\lambda = 151$ and 164 μm in the intermediate range of electric fields (Fig. 5) where the amalgamation of the lower- and the higher-field domains takes place (Fig. 7). In addition, the emission lines in the longer-wavelength range ($\lambda > 170$ μm) and those in the shorter-wavelength range ($\lambda < 120$ μm) coexist in the intermediate range of E at 450 kg/cm^2.

IV. DISCUSSION AND INTERPRETATION

Uniaxial stress is known to remove the degeneracy of the light- and the heavy-hole bands at $\mathbf{k}=\mathbf{0}$.[11] The energy spectra of the respective bands were calculated for [112] compressive stress of $F=450$ kg/cm^2 according to the theory of Pikus and Bir and are shown in Fig. 8(a). The parameters used for the calculation are as follows: the elastic compliance constants,[18] $S_{11}=9.37\times10^{-7}$ cm^2/kg, $S_{12}=-2.57\times10^{-7}$ cm^2/kg, and $S_{44}=14.3\times10^{-7}$ cm^2/kg; the deformation potential constants,[19] $b=-2.21$ eV and $d=-4.40$ eV; the effective-mass parameters,[19] $A=-13.38$, $B=-8.48$, and $D=-19.71$ in unit of $\hbar^2/2m_0$. Specifically, the energy splitting $2\Delta_{112}$ between the bands at $\mathbf{k}=\mathbf{0}$ is written as

$$2\Delta_{112}=\{[4b^2(S_{11}-S_{12})^2+d^2S_{44}^2]^{1/2}/2\}F$$
$$=4.1\times10^{-6}F \text{ eV}$$

for [112] stress, which is evaluated to be 1.85 meV at $F=450$ kg/cm^2.[20]

There are several possible mechanisms through which the stress may influence the laser oscillation. Firstly, the trajectories of free motion of holes in external fields may be modified because the energy spectra are modified. However, this is not likely to significantly influence the overall characteristics of the laser oscillation because the region in k space where the energy spectra are significantly modified is limited to a relatively narrow region around $\mathbf{k}=\mathbf{0}$ at the stress values presently adopted as shown in Fig. 8(a), while the holes traverse the larger energy region below $\varepsilon=\hbar\omega_{op}$. Second, the matrix elements for the intervalence-band optical transition may be modified. When the character of the stress-induced changes of the wave functions of holes is considered,[11] the dependence of the matrix elements on the light polarization is expected to alter significantly, as is confirmed experimentally for the transition between the heavy-hole band and the spin-orbit-split band.[21] However, the magnitudes of the matrix element averaged over different polarization directions do not vary significantly and this mechanism is also not likely to be the major origin here. Third, the rate of holes supplied to the light-hole band after the optical phonon emission by heavy holes may be reduced, because the bottom of the light-hole band is lifted by $2\Delta_{112}$ from that of the heavy-hole band. However, this effect is also supposed to be insignificant because the average kinetic energy possessed by the holes after the optical phonon emission $\bar{\varepsilon}=0.19E^{2/3}$ meV,[22] reaches as high a value as 7.6 meV even at $E=260$ V/cm and because, as this may be more important, the density-of-state

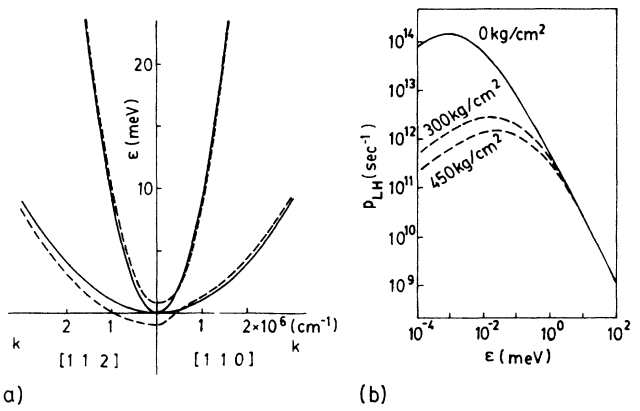

FIG. 8. (a) The energy spectra of light and heavy holes in Ge subjected to the [112] stress of magnitude 450 kg/cm^2 (dashed lines). The solid lines indicate the spectra in zero stress. (b) The probability of the transition of light holes to the heavy-hole band, $P_{\rm LH}$, due to ionized impurity scattering, as a function of the kinetic energy of light holes. The probability $P_{\rm LH}$ decreases remarkably when uniaxial stress F is applied.

mass of light holes in the vicinity of $\mathbf{k}=0$ increases to approximately compensate the effect of the energy splitting. Finally, the most probable mechanism is a reduction in the rate of the interband impurity scattering as discussed in the following.

Before discussing the effect of uniaxial stress, we consider the characteristics of the interband impurity scattering and their influence on the laser oscillation in the absence of stress. In the present laser oscillation the population inversion is caused by the accumulation of light holes in crossed electric and magnetic fields.[23,24] In the condition of $\zeta_h \sim 1.3$ [relation (1)], heavy holes frequently emit optical phonons, while light holes have a relatively long lifetime being free from the phonon emission. Aside from the rate of the optical phonon emission by heavy holes, the degree of the light-hole accumulation is determined by the lifetime of light holes. This lifetime is limited by the light-hole transitions to the heavy-hole band, which are caused by the acoustical phonon scattering, the electric-field-induced tunneling,[25,26] and the ionized impurity scattering. Among these processes, the ionized impurity scattering is supposed to be the most dominant process in the experimental conditions, since (1) an evaluation of the acoustical phonon scattering can prove it to be insignificant in comparison to the ionized impurity scattering and (2) a systematic increase of the degree of light-hole accumulation with increasing sample purity in the range $N_a = 3\times10^{13}-2\times10^{14}$ cm^{-3} has been observed in experimental studies of the spontaneous inter-valence-band emissions.[27] The probability for light holes to be scattered to the heavy-hole band due to ionized impurities in the absence of stress, $P_{\rm LH}$, is calculated for the impurity concentration of $N_a = 6\times10^{13}$ cm^{-3} according to Ref. 28 and is shown as a function of the light-hole kinetic energy ε with a solid line in Fig. 8(b).[29] The probability $P_{\rm LH}$ is anomalously high in an extremely low-energy range ($\varepsilon \sim 1\times10^{-3}$ meV) because the momentum change involved in the scatterings can be vanishingly small as ε approaches to zero while the screening effect on the scatterings is not very significant for $\varepsilon > 10^{-3}$ meV in the present experimental condition. Because of this singularity of $P_{\rm LH}$, the population of light holes on the trajectories passing near the point $\mathbf{k}=0$ is expected to be severely suppressed, as also pointed out theoretically by Kozlov *et al.*[30] The ring-shaped region in k space where such "empty" trajectories are located are schematically shown with a shaded area in Fig. 9 for the case of $\zeta_h = 1.3$.[31] To consider the emissions of photons with wavelength λ through the direct optical transition to the heavy-hole band, we imagine in k space the equienergy sphere with the radius k_λ given by

$$hc/\lambda = (\hbar^2 k_\lambda^2/2m_l^*)(1 - m_l^*/m_h^*) ,$$

where $m_l^* = 0.043 m_0$ is the light-hole effective mass. The sphere, $k = k_\lambda$ constitutes the initial states for the transition. It can be easily shown that, in the optimum conditions of $\zeta_h = 1.2-1.4$, the "empty" region is tangent to the sphere when $\lambda = 110-150$ μm. Therefore the characteristics of the laser oscillation are expected to be different according as $\lambda \gtrsim 150$ μm or $\lambda \lesssim 110$ μm. The gain coefficients for the radiations with $\lambda \gtrsim 150$ μm may be relatively small and their magnitudes may depend sensitively on the impurity concentration, since the sphere representing the initial states intersects the empty region [Fig. 9(a)], while they may be relatively high, independently of the impurity concentration, for the wavelengths shorter than 110 μm, since the initial states are separated from the empty region [Fig. 9(b)]. Furthermore, the gain may be lowest for the wavelengths 110–150 μm. This picture, when combined with the additional theoretical prediction that the photon energy at which the maximum gain is attained is an increasing function of electric field,[8] substantially accounts for all the observed characteristics of the laser oscillation in the absence of stress.[32] Although the gap range of λ (120–170 μm), where the oscillation is missing in the experiments, is in slight disagree-

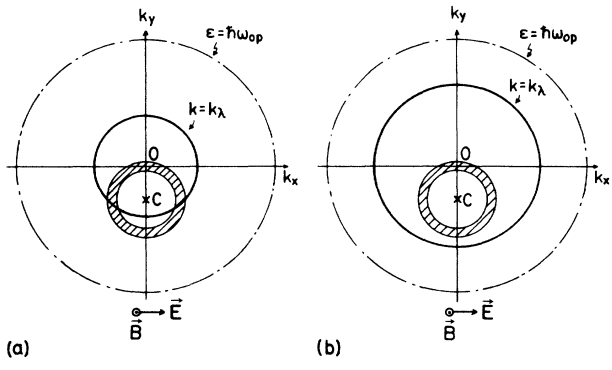

FIG. 9. The trajectories of cyclotron orbits of light holes passing near $\mathbf{k}=0$ at $\zeta_h = 1.3$ and the equienergy sphere $k = k_\lambda$. The center of the cyclotron orbits is point C $(0, m_l^* E/\hbar B)$. The sphere $k = k_\lambda$ indicates the initial states for the interband optical transition yielding the emission of wavelength λ. (a) For $\lambda > 150$ μm, the equienergy sphere intersects the trajectories passing near $\mathbf{k}=0$. (b) for $\lambda < 110$ μm, the sphere is separated from the trajectories.

ment with the expected range 110–150 μm, the arguments above may not be precise enough for the discrepancy of this amount to be quantitatively discussed.

When uniaxial stress is applied to remove the valence-band degeneracy at $\mathbf{k}=\mathbf{0}$, the probability P_{LH} in the low-energy range decreases remarkably because a finite momentum change is necessarily involved in the scattering process even at $\mathbf{k}=\mathbf{0}$. The amplitudes of P_{LH} in the presence of the valence-band splitting have been roughly estimated and are compared with the stress-free values in Fig. 8(b).[33] According to the results shown in Fig. 8(b), the probability $\bar{P}_{\mathrm{LH}}$ averaged over the circular trajectory passing $\mathbf{k}=\mathbf{0}$ is reduced by about 1 order of magnitude at any stress value of 300 and 450 kg/cm^2. Accordingly, the population of light holes in the ring-shaped empty region will increase significantly, making the oscillations in the longer- and the shorter-wavelength ranges equally feasible. This explains the experimental observations that (1) the intensity of the longer-wavelength oscillations ($\lambda > 170$ μm) increases to a level comparable to that of the shorter-wavelength oscillations, (2) the intensity of the shorter-wavelength oscillations ($\lambda < 120$ μm) does not change significantly, (3) the oscillation domains of the longer and the shorter wavelengths nearly merge with each other at stress value 450 kg/cm^2, and (4) new oscillation lines ($\lambda = 151$ and 164 μm) appear in the intermediate-field range at stress value 450 kg/cm^2. In addition, the reduction of the threshold electric fields for the oscillations is naturally interpreted as a consequence of the increase of the light-hole population.

Although the dominant features of the oscillation in uniaxial stress have thus been reasonably interpreted, there are a few experimental results which are not accountable within our simple picture. For instance, the physical origin of the pronounced structure appearing in the signal versus B curves (Fig. 3) is not clear. The narrowing of the higher-field domain near the neck region at stress magnitude 300 kg/cm^2 (Fig. 6) is also not explained. For the interpretation of these detailed features, an advanced analysis of the effects of uniaxial stress may be necessary.

It is to be noted that the inter-valence-band impurity scattering is extremely sensitive to the application of uniaxial stress as discussed above but the intraband impurity scattering is not so. This is the reason why the laser oscillations are influenced so significantly by the uniaxial stress while the current-voltage characteristics are substantially unaffected. It is also to be pointed out that the remarkable effects of uniaxial stress are expected independently of the stress orientation, since the valence-band splitting is a consequence of the reduction of the cubic symmetry of the crystal and the magnitudes of the splitting do not differ very much for different stress orientations.[20] The uniaxial stress is expected to be more effective for the samples with higher acceptor concentrations since it makes the ionized impurities ineffective as scatterers while keeping unchanged the density of carriers, which is equal to the acceptor concentration. Specifically, the longer-wavelength oscillation ($\lambda > 170$ μm) has not been reported in the samples with $N_a > 1.0\times10^{14}$ cm^{-3} (Refs. 4, 5, and 34) but we expect it to arise when uniaxial stress is applied.

The electric-field-induced tunneling of light holes to the heavy-hole band[25,26] is expected to become increasingly important as the acceptor concentration in the samples decreases. Since the tunneling also occurs primarily in a low-energy range near the degenerated point $\mathbf{k}=\mathbf{0}$ under the restriction of the energy conservation, the probability of the tunneling is again expected to decrease when the degeneracy is removed by uniaxial stress. Hence uniaxial stress may be also useful to enhance the light-hole accumulation in purer samples.

V. SUMMARY

Studies of the inter-valence-band far-infrared laser oscillation in p-type Ge subjected to [112] uniaxial stress have been reported. In zero stress, the region of electric and magnetic fields where the oscillation takes place is divided into the lower- and the higher-field domains with the border at $E \sim 800$ V/cm and $B \sim 5.5$ kG. The lower-field domain is characterized by the longer-wavelength oscillation ($\lambda > 170$ μm) and the higher-field domain is characterized by the shorter-wavelength oscillation ($\lambda < 120$ μm). At stress magnitudes 300±70 and 450±80 kg/cm^2, the lower-field domain extends remarkably to lower fields and the intensity of the laser emission there increases by a factor $10-10^3$. On the other hand, the emission intensity does not change remarkably in the higher-field domain. Further, the lower- and the higher-field domains tend to merge with each other at stress magnitude 450±80 kg/cm^2 and new emission lines appear at intermediate wavelengths (151 and 164 μm).

To interpret the experimental results, it is pointed out that the rate of the inter-valence-band impurity scattering, which occurs dominantly in the vicinity of $\mathbf{k}=\mathbf{0}$, is remarkably reduced when uniaxial stress is applied to remove the band degeneracy. The experimental results are interpreted as a consequence of the resulting increase of the light-hole accumulation. It is pointed out that the tunneling transition of light holes to the heavy-hole band is also suppressed to help the laser oscillation under uniaxial stress. Thus, the application of uniaxial stress is a useful and powerful tool to promote the accumulation of light holes and the characteristics of the laser oscillation are, generally, expected to be thereby largely improved.

ACKNOWLEDGMENTS

We are grateful to T. Ohyama and E. Otsuka at Osaka University for useful advice about the techniques of stress application. This work is supported by the Grant-in-Aid for Developmental Scientific Research from the Ministry of Education, Science and Culture.

[1]A. A. Andronov, I. V. Zverev, V. A. Kozlov, Yu. N. Nozdrin, S. A. Pavlov, and V. N. Shastin, Pis'ma Zh. Eksp. Teor. Fiz. **40**, 69 (1984) [JETP Lett. **40**, 804 (1984)].

[2]S. Komiyama, N. Iizuka, and Y. Akasaka, Appl. Phys. Lett. **47**, 958 (1985).

[3]A. V. Murav'ev, Yu. N. Nozdrin, and V. N. Shastin, Pis'ma Zh. Eksp. Teor. Fiz. **43**, 348 (1986) [JETP Lett. **43**, 449 (1986)].

[4]A. A. Andronov, A. V. Murav'ev, I. M. Nefedov, Yu. N. Nozdrin, S. A. Pavlov, V. N. Shastin, Yu. A. Mityagin, V. N. Murzin, S. A. Stoklitsky, I. E. Trofimov, and A. P. Chebotarev, in *Proceedings of the 18th International Conference on the Physics of Semiconductors, Stockholm, 1986,* edited by O. Engström (World Scientific, Singapore, 1986), p. 1663.

[5]S. Komiyama, in *Proceedings of the 18th International Conference on the Physics of Semiconductors,* Ref. 4, p. 1641.

[6]S. Komiyama and S. Kuroda, Jpn. J. Appl. Phys. **26**, L71 (1987).

[7]S. Komiyama, S. Kuroda, and T. Yamamoto, J. Appl. Phys. **62**, 3552 (1987).

[8]A. A. Andronov, A. M. Belyantsev, E. P. Dodin, V. I. Gavrilenko, Yu. L. Ivanov, V. A. Kozlov, Z. F. Krasil'nik, L. S. Mozov, A. V. Muravjov, I. M. Nefedov, V. V. Nikanorov, Yu. N. Nozdrin, S. A. Pavlov, V. N. Shastin, V. A. Valov, and Yu. B. Vasil'ev, Physica B&C **134B**, 210 (1985).

[9]S. Komiyama and S. Kuroda, Solid State Commun. **59**, 167 (1986).

[10]Yu. A. Mitjagin, A.V. Murav'ev, V. N. Murzin, Yu. N. Nozdrin, S. A. Pavlov, S. A. Stoklitsky, I. E. Trofimov, A. P. Chebotarev, and V. N. Shastin, Kratk. Soobshch. Fiz. **12**, 30 (1986).

[11]G. E. Pikus and G. L. Bir, Fiz. Tverd. Tela (Leningrad) **1**, 1642 (1958) [Sov. Phys.—Solid State **1**, 1502 (1960)].

[12]A. G. Kazanskii, P. L. Richards, and E. E. Haller, Appl. Phys. Lett. **31**, 496 (1977).

[13]J. Léotin, C. Laverny, M. Goiran, S. Askénagy, and J. R. Birch, Int. J. Infrared Millimeter Waves **6**, 323 (1985).

[14]J. J. Hall, Phys. Rev. **128**, 68 (1962).

[15]Y. Oka, K. Nagasaka, and S. Narita, Jpn. J. Appl. Phys. **7**, 148 (1968).

[16]The spectral responsivity of Ge/Sb detectors depends sensitively on the detector bias current I as states in Ref. 2. In the experiments, $I \simeq 5\ \mu$A was applied.

[17]S. Komiyama and S. Kuroda (unpublished).

[18]H. J. McSkimin, J. Appl. Phys. **24**, 988 (1953).

[19]J. C. Hensel and K. Suzuki, Phys. Rev. B **9**, 4219 (1974).

[20]The energy splittings 2Δ for [100], [110], and [111] stress orientations are, respectively, $5.28\times10^{-6}F$ eV, $4.11\times10^{-6}F$ eV, and $3.63\times10^{-6}F$ eV, where F is in units of kg/cm^2.

[21]I. Balslev, Phys. Rev. **177**, 1173 (1969).

[22]I. B. Levinson, Usp. Fiz. Nauk. **139**, 347 (1983) [Sov. Phys.—Usp. **26**, 176 (1983)].

[23]A. A. Andronov, V. A. Kozlov, L. S. Mazov, and V. N. Shastin, Pis'ma Zh. Eksp. Teor. Fiz. **30**, 585 (1979) [JETP Lett. **30**, 551 (1979)].

[24]S. Komiyama, Adv. Phys. **31**, 255 (1982).

[25]B. M. Gorbovitskii, Fiz. Tekh. Poluprovodn. **18**, 704 (1984) [Sov. Phys.—Semicond. **18**, 437 (1984)].

[26]V. Ya. Aleshkin and Yu. A. Romanov, Fiz. Tekh. Poluprovodn. **20**, 281 (1986) [Sov. Phys.—Semicond. **20**, 176 (1986)].

[27]N. Iizuka, Master thesis, Tokyo University, 1985 (unpublished).

[28]M. Costato and L. Reggiani, Phys. Status Solidi B **58**, 471 (1973).

[29]In the calculation of the hot carriers there is an ambiguity in the choice of the Debye's screening length. We have adopted the cutoff parameter $L = 2N_a^{1/3}$ as the screening length. However the overall feature of $P_{\rm LH}(\varepsilon)$ is almost unaffected by the different choice of L.

[30]V. A. Kozlov, L. S. Mazov, I. M. Nefedov, and M. R. Zabolotskikh, Pis'ma Zh. Eksp. Teor. Fiz. **37**, 142 (1983) [JETP Lett. **37**, 170 (1983)].

[31]Precisely, the trajectories passing near $\mathbf{k}=\mathbf{0}$ are not empty, because the probability of the transition of heavy holes to the light-hole band is equally high at $\mathbf{k}\sim\mathbf{0}$. However, the population on these trajectories in the equilibrium state is relatively much lower than that on the other trajectories.

[32]To account for the characteristics of the laser oscillation discussed here, Murav'ev, Nozdrin, and Shastin considered in Ref. 3 discrete semiclassical Landau orbits of light holes together with the anomaly of the light-hole lifetime at $\mathbf{k}\sim\mathbf{0}$. However, we can show that the effect of Landau quantization is likely to be irrelevant to the observed behavior of the oscillation wavelengths, by considering the harmonic-oscillator-type wave functions for the Landau states. Hence we suppose that the completely classical picture, described here, is more appropriate.

[33]To estimate $P_{\rm LH}$ under uniaxial stress, we have replaced the screening length L by the inverse of the minimum wavenumber change $(\Delta k)^{-1} \equiv (\hbar/2)(m_h^* \Delta_{112})^{-1/2}$ for the scattering at $\mathbf{k}=\mathbf{0}$ in the presence of the energy splitting $2\Delta_{112}$. We have made the replacement only in the prefactor A of the probability $P_{\rm LH} = AG_{\rm LH}$, where we have kept $G_{\rm LH}$, the term arising from the overlap integral, unchanged.

[34]M. Helm, K. Unterrainer, E. Gornik, and E. E. Haller, in Proceedings of the 5th International Conference on Hot Carriers in Semiconductors, Boston, 1987 (unpublished).